Polymer Degradation and Stability 240 (2025) 111482

Contents lists available at ScienceDirect

Polymer Degradation and Stability

journal homepage: www.journals.elsevier.com/polymer-degradation-and-stability

Improvement of mechanical and thermal properties of epoxy composites with citric acid modified and defibrated cellulose filler

Shotaro Yano, Yu-I Hsu *, Hiroshi Uyama *

Department of Applied Chemistry, Graduate School of Engineering, Osaka University, 2-1 Yamadaoka, Suita, Osaka, 565-0871, Japan

ARTICLE INFO

Keywords:
Cellulose
Citric acid modification
Defibration
Epoxy resin
Composite

ABSTRACT

Cellulose is a biomass filler with low environmental impact; however, its application presents challenges such as poor affinity between hydrophobic plastics and hydrophilic cellulose and the aggregation of cellulose. In this study, citric acid-modified cellulose (CAC) was used as an environment-friendly filler for enhancing the mechanical properties of epoxy composites. CAC was prepared via the esterification of cellulose with citric acid. In addition, a defibrated CAC (F-CAC) with a fiber diameter of ~140 nm was produced using a grinder. The addition of F-CAC doubled Young's modulus increased it from 1.07 GPa to 2.08 GPa, and raised the glass transition temperature by 1.8 °C. The microscopic observations of composites revealed that CAC demonstrated a greater affinity for matrix than that of unmodified cellulose, whereas F-CAC exhibited enhanced dispersibility within the composites. Carboxyl groups introduced during the citric acid-modification may have contributed to the interaction between the filler and epoxy network. The incorporation of CAC or F-CAC as fillers improved the mechanical and thermal properties of epoxy composites. This research expands the range of applications for CAC, an environmentally friendly filler. It is anticipated that CAC will facilitate the development of high-strength, low-environmental-impact epoxy.

1. Introduction

Epoxies synthesized from epoxides and curing agents are categorized as thermosetting resins and recognized for their excellent performance in terms of mechanical strength, toughness, and chemical and thermal resistance [1]. These attributes are crucial for their versatile applications in coatings, electronics, construction materials, and adhesives [2,3]. Chemically, a three-membered ring of epoxide forms a covalent bond with a curing agent molecule via a ring opening, and the curing agent molecule and epoxide react continuously, building a three-dimensional network. In industry, bisphenol-A (BPA) diglycidyl ether (DGEBA), which contains epoxides at both ends, is the most commonly used epoxy resin (ER) [4,5]. When a specific performance characteristic such as low viscosity or heat resistance is desired, double-ended epoxides with different molecular structures are used alone or in combination with DGEBA [6,7]. However, DGEBA is produced from petroleum-derived BPA and epichlorohydrin. Their ongoing utilization and the resultant depletion of nonrenewable resources in the mass production of epoxies have prompted environmental concerns, with greenhouse gas emissions contributing to climate change and global warming [8].

Epoxies are not biodegradable, and once they spill into the ocean, the plastic remains crushed. Therefore, from the perspective of the sustainable development goals proposed by the United Nations, a solution to this problem is urgently required. Consequently, there is growing interest in bio-based epoxies that leverage renewable resources to mitigate their environmental impact [9]. These bio-based epoxies incorporate biomass components [10] such as lignin [11] and vanillin [12] derived from lignin, gallic acid [13], sorbitol [14,15], and isosorbitol [16]. For example, lignin, which is a natural aromatic polymer, is epoxidized using bio-based epichlorohydrin to produce epoxies. Vanillin can be synthesized from lignin, which contains an alcohol substituted for an aromatic ring and alcohol in the benzyl position. Vanillin is epoxidized with epichlorohydrin to produce a completely bio-based epoxy [17]. However, their current commercial use is limited by their strength, which is comparable to that of conventional resins.

To address these issues, fillers have been extensively integrated into resins to enhance their strength. Typical fillers such as glass [18] and carbon fibers [19,20] pose challenges in terms of recovery, post-composite processing, and disposal, exacerbating environmental burdens. Eco-friendly alternatives have gained considerable attention as

* Corresponding authors.
E-mail addresses: yuihsu@chem.eng.osaka-u.ac.jp (Y.-I. Hsu), uyama@chem.eng.osaka-u.ac.jp (H. Uyama).

https://doi.org/10.1016/j.polymdegradstab.2025.111482
Received 3 March 2025; Received in revised form 9 June 2025; Accepted 10 June 2025
Available online 11 June 2025

replacements for traditional fillers to alleviate these issues, with cellulose being a promising candidate [21]. Cellulose, which is a naturally abundant fiber, has a chain structure that comprises a six-membered ring of glucose dehydrated and condensed by hydroxyl groups at positions C1 and C4 [22]. This intricate arrangement imparts notable properties to cellulose, including structural strength [23], biocompatibility, and lightweight [24]. These characteristics promote the industrial use of cellulose as a renewable resource. In the field of materials, there are high expectations for using cellulose as a raw material or filler to produce materials with higher biomass resources and lower environmental impact [25]. However, despite these advantageous qualities, the hydrophilic nature and limited affinity [26] of cellulose for resins by three hydroxy groups per glucose unit, which is attributed to the numerous hydroxyl groups and hydrogen bonding, hinder its dispersibility and application as a filler [27].

Thus far, various types of modified cellulose have been reported, including 2,2,6,6-tetramethylpiperidine-1-oxyl (TEMPO) oxidized cellulose nanofibers (TOCF) [28] and cellulose nanocrystals (CNC) [29]. In TOCF, the hydroxyl group at the C6 position of cellulose is oxidized to a carboxyl group by the oxidants TEMPO and sodium hypochlorite [30]. The sodium salt of the carboxyl group at the C6 position inhibits hydrogen bonding, enabling the easy preparation of nanofibers. Although TOCF exhibits high strength as nanofibers, TEMPO is expensive, and TOCF has low recovery as well as long oxidation times [31]. CNCs, on the other hand, are crystalline colloids obtained by heat-treating cellulose with sulfuric or other acids [32]. Their addition can improve the strength and water-barrier performance of the composites; however, their intricate synthetic processes and reliance on toxic reagents hinder their widespread industrial applications [33]. As such, ongoing research is directed toward the development of modified cellulose fibers with a simpler and greener production to serve as a filler for epoxies.

Ma and Webster have previously investigated the use of water-soluble natural acids, namely citric acid (CA), which acted as a cross-linker in their epoxidized sucrose soybean system [34]. It was found that with the excellent water solubility of CA, the cross-linking occurred very rapidly along with the main ring-opening reaction during the curing process. On top of this, the resulting thermoset could fully degrade with aqueous sodium hydroxide solutions, making them fully green [34]. A study by Kocaman, Ahmetli & Temiz found that adding CA into an epoxy resin with almond shell waste filler (mixture of cellulose, hemicellulose, and lignin) could elevate the adhesion between them and their resultant tensile strengths [35]. In a previous study, a method for modifying cellulose through esterification with CA was found to be environmentally conscious, given that CA-modified cellulose (CAC) can be synthesized easily by amalgamating cellulose and CA in an aqueous medium, followed by a heating process [36]. The degree of substitution of the hydroxyl groups of cellulose by esterification can be controlled by varying the heating conditions [37]. Carboxyl groups introduced into CAC have been reported to improve their compatibility with polylactic acid and the bending properties of composites [38]. In addition, CAC can be modified with magnesium stearate to improve its compatibility with polyesters by grafting alkyl chains, which improves the tensile properties of the composites [39].

In this study, cellulose was modified with CA and defibrated to improve the mechanical properties of epoxy composites. Defibrated CAC (F-CAC) was composited with the epoxide 1,6-hexanediol diglycidyl ether (HDDGE) (Fig. 1). The influence of the addition of CAC as a filler on the mechanical and thermal properties of the composites was investigated by comparing untreated cellulose, CAC, and F-CAC composites.

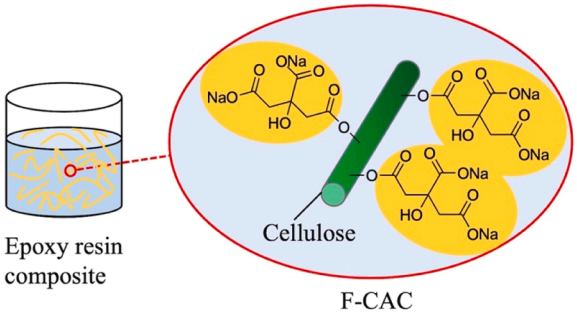

Fig. 1. Illustration of the epoxy resin composite with F-CAC from cellulose.

2. Experimental section

2.1. Materials

Cellulose powder (Nacalai Tesque Corporation, Kyoto, Japan) and citric acid powder (FUJIFILM Wako Pure Chemical Corporation, Osaka, Japan) were used to prepare CAC. For neutralization titration, 0.05 mol/L sodium hydroxide solution (Nacalai Tesque Corporation, Kyoto, Japan) and 1 mol/L hydrochloric acid (Nacalai Tesque Corporation, Kyoto, Japan) were used. A sodium hydroxide solution (1 and 8 mol/L; Nacalai Tesque Co., Ltd., Kyoto, Japan) was used for neutralizing CAC before defibration.

Epoxies (composites) were prepared using HDDGE (Nagase ChemteX Corporation, Osaka, Japan), 4-methylcyclohexane-1,2-dicarboxylic anhydride (MHHPA) (Tokyo Chemical Industry Co., Ltd., Tokyo, Japan), and tetraethylammonium bromide (TEAB) (FUJIFILM Wako Pure Chemicals Corporation, Osaka, Japan). Deionized water (DIW) was purified using a Milli-Q. Methanol and acetone were purchased from the FUJIFILM Wako Pure Chemical Corporation. All reagents were used without further purification.

2.2. Synthesis and defibration of CAC

CA (90 g) was added to 200 mL of DIW and stirred with magnetic stirring at room temperature for 15 min. Next, 30 g of cellulose powder was added, and the mixture was stirred at room temperature for 30 min. Then, the dispersion was heated in an oven at 130 °C for 13 h with the container lid open, which resulted in CAC by esterification (Table 1) (Fig. 2). CAC was neutralized, and any unreacted components were removed by washing with DIW. CAC-1.0 powder was obtained after washing with 500 mL of methanol and 300 mL of acetone, followed by vacuum drying. The same procedure was used for preparing CAC-2.1 by heating at 140 °C for 15 h. After heating at 140 °C for 15 h by the same procedure, 200 mL of DIW was added to the unrefined CAC to prepare a dispersion solution, which was again heated at 140 °C for 15 h. Following the third heating, this resulted in CAC-2.7, which was then purified using the same procedure. Each powder was stored in an airtight compartment at room temperature.

CAC (0.4 g) was added to 200 mL of DIW, stirred with magnetic stirring, and the pH was adjusted to 2.5–3.0 by adding 1 mol/L hydrochloric acid. Then, 0.05 mol/L sodium hydroxide solution was added in 0.3 mL increments, and the pH and conductivity of CAC dispersion were measured using a pH and conductivity meter. With the addition of the

Table 1
Conditions for CAC synthesis.

	Temp. [°C]	Time [h]	Heating cycle [times]	Introduced carboxyl group [mmol/g]
CAC-1.0	130	13	1	1.0
CAC-2.1	140	15	1	2.1
CAC-2.7	140	15	3	2.7

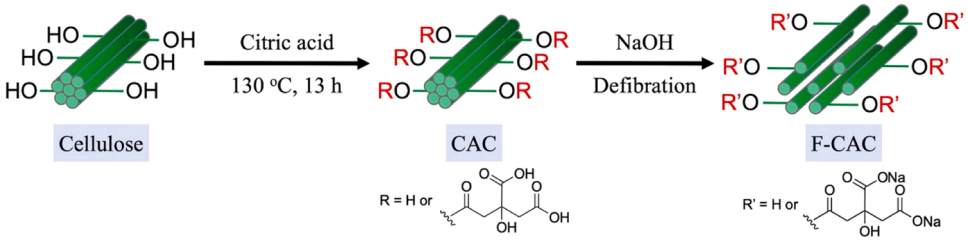

Fig. 2. Illustration of the synthesis of CAC and F-CAC from cellulose.

sodium hydroxide solution, the electrical conductivity decreased, plateaued, and then increased. The number of carboxyl groups introduced was calculated from the drop volume and concentration of the sodium hydroxide solution, while the electrical conductivity showed a plateau.

The obtained CAC powder was placed in DIW to form a CAC dispersion and adjusted to pH 8.5–9.0 using 1 and 8 mol/L sodium hydroxide solutions. The alkaline CAC was collected after three rounds of centrifugation and washing. This alkaline CAC was then defibrated using a Supermasscolloider (Masuko Sangyo, Saitama, Japan) with 15 passes at 1200 rpm and squeezed to the 25th scale to obtain an F-CAC dispersion. The powdered F-CAC was recovered after ultrasonication for 1 h, followed by lyophilization and pulverization (Lab Mill; Osaka Chemical Co., Ltd., Osaka, Japan). F-CAC powder was stored in an airtight compartment at room temperature.

2.3. Preparation of epoxy composites

The epoxy group (15 mmol) from HDDGE was added to the reaction vessel, along with MHHPA (21 mmol) and TEAB (0.105 mmol). The subsequent ratio would be 1:2.8:0.007 of epoxide to the carboxyl group on the catalyst. From the weight of reagents added, the filler was added at 1, 3 or 5 wt % of the total and was stirred with magnetic stirring under vacuum for 1 h. The fillers used in this study were untreated cellulose, defibrated cellulose (F-Cellulose), CAC, and F-CAC. The resulting solution was transferred to an aluminum mold and degassed under vacuum for 3 h. The mold would then be heat cured in a sealed oven at 150 °C for 3 h to obtain the composites, **Neat ER, Cellulose/ER, F-Cellulose/ER, CAC/ER**, and **F-CAC/ER**.

For composites with 10 or 15 wt % filler, the reagent and filler were added, and the mixture was stirred for 5 min in a planetary centrifugal mixer (Awatori Rennntaro AR-100, Shinky Corporation, Tokyo, Japan). Subsequently, the mixture was agitated under vacuum, degassed, and heated.

2.4. Characterization

2.4.1. Fourier transform infrared spectroscopy (FT-IR)

The FT-IR (Nicolet iS5 Spectrometer, Thermo Fisher Scientific Corporation, Tokyo, Japan) was used to confirm the modification by CA. Measurements were made in the wavenumber range of 400–4000 cm^{-1}.

2.4.2. Morphology

Scanning electron microscopy (SEM, SU3500, Hitachi High-Tech, Tokyo, Japan) was used to observe morphology, operating at 5.0 kV with 3 nm platinum sputter coating. Samples for cross-sectional observation were prepared by immersing the composites in liquid nitrogen for 10 s and then breaking them off.

2.4.3. Titration

The pH meter (LAQUA F-74; HORIBA, Ltd., Osaka, Japan) was used for titration. The number of carboxyl groups on the cellulose surface was quantified by electrical conductivity titration using an aqueous sodium hydroxide solution (See Chapter 2–2 for details).

2.4.4. Mechanical property

The mechanical properties of the composites were determined using a tabletop material-testing machine (EZ Graph; Shimadzu Corporation, Kyoto, Japan) for tensile testing. The composites were cut into dumbbell pieces (type 7) for testing, and the average value and standard deviation were calculated from the results of five dumbbell pieces. A 500 N load cell was used, the distance between the gripping fixtures was 10 mm, and the tensile speed was 10 mm/min.

2.4.5. Thermal property

Dynamic mechanical analysis (DMA, DMA7100, Hitachi High-Tech Corporation, Tokyo, Japan) was used for the thermal analysis. Measurements were performed in tensile mode, with 20 mm between holders. Thermal conditions ranged from −30 to 130 °C, with a temperature increase rate of 3 °C/min and a sampling time of 3 s.

3. Results and discussion

3.1. Synthesis of CAC and F-CAC

Cellulose was added to the CA solution and heated at 130 °C for 13 h to allow esterification. CAC was prepared under three different temperatures and time conditions for esterification (Table 1). The initial cellulose was a white powder. After CA-modification, the obtained CAC was a light-yellow powder (Fig. 3a-d). According to the FT-IR results for CAC with cellulose, a new peak appeared at 1727.9 cm^{-1}, indicating the $C=O$ stretching vibration of CA, thereby confirming the introduction of carboxyl groups into CAC (Fig. 4) [40]. Subsequently, the number of introduced carboxyl groups was calculated from the conductivity titration against sodium hydroxide as done by Masruchin &Park (2015) [41], to further verify the change in the introduced carboxyl groups in different heating conditions. The higher the reaction temperature or the longer the reaction time, the more carboxyl groups were introduced. CAC-2.7 was prepared by heating the dispersion, in which DIW was added back to CAC immediately after the completion of heating for a total of three heating cycles. With an increase in the number of heating cycles, the number of carboxyl groups introduced increased correspondingly.

F-CAC was synthesized via the defibration of CAC. Comparison of CAC and F-CAC was analyzed via SEM, and the images showed a reduction in the fiber diameter from 10 μm to 140 nm followed by an increase in the aspect ratio after defibration (Fig. 3e-f).

3.2. Dispersibility of CAC and F-CAC as a filler

Composites with untreated cellulose, F-Cellulose, CAC, and F-CAC as fillers were prepared along with epoxy without a filler as control, and then, they were lyophilized to analyze their morphologies (Fig. 5a–5o). The epoxy without filler (**Neat ER**) was clear and colorless, with a smooth fracture surface (Fig. 5a–5c). However, on adding cellulose to the epoxy, the composite (**Cellulose/ER**) turned white (Fig. 5d–5f). From the cross-section, the filler was not dispersed uniformly but accumulated on one side because of the possible aggregation and precipitation of the cellulose filler during the degassing process. Further,

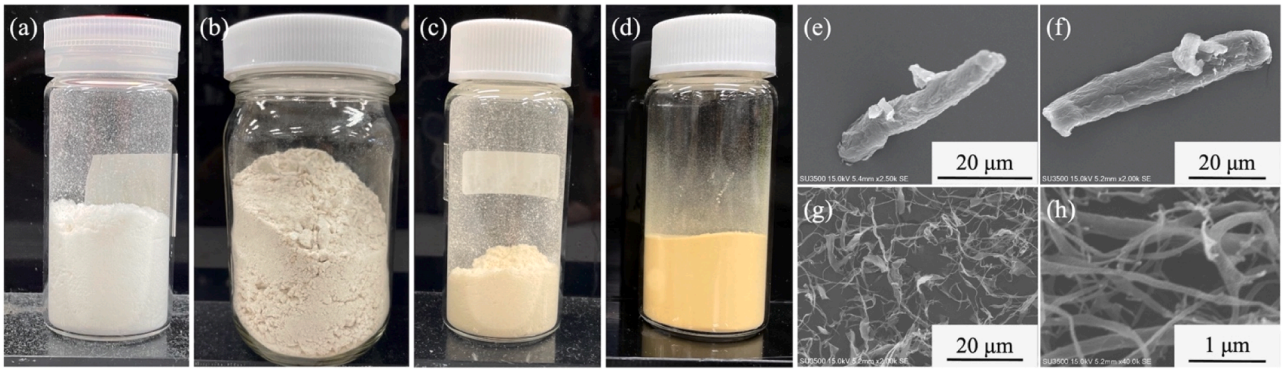

Fig. 3. Pictures of (a) Cellulose, (b) CAC-1.0, (c) CAC-2.1, (d) CAC-2.7. SEM images of (e) Cellulose, (f) CAC-1.0, and (g, h) F-CAC-1.0.

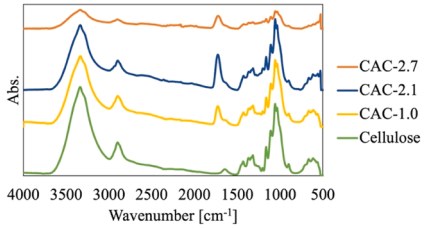

Fig. 4. Fourier transform infrared spectra of fillers.

there was an apparent separation between the cellulose filler and the matrix, which suggests the inability of the filler and matrix to adhere and homogenize. This can be attributed to the hydrophilicity of cellulose from its surface hydroxyl groups, which contributes to its low affinity for the matrix.

The **F-Cellulose/ER** using defibrated cellulose as a filler showed a white color caused by F-Cellulose (Fig. 5g-5i). The cross-section shows that F-cellulose was dispersed throughout the composite. F-cellulose suppresses precipitation and improves dispersion because the fiber diameter of cellulose decreases owing to defibration.

However, in the **CAC/ER**, the composite was partly tinted a slight yellow compared to CAC (Fig. 5j–5l). Observation of the cross-section confirmed that CAC was accumulated on one side (red square in Fig. 5k). On the other hand, CAC adhered to the matrix better than cellulose, verifying the improved affinity of the filler to the matrix. With the CA-modification, the number of hydroxyl groups decreased, whereas the number of carboxyl groups increased. Similar results were obtained for all the CAC composites (CAC-1.0, 2.1, and 2.7).

Furthermore, with the defibrated filler in the **F-CAC/ER** composite, the yellow color was well-dispersed, which was in agreement with the cross-section that showed a uniform distribution (Fig. 5m–5o). The decrease in the fiber diameter improved the dispersibility of the filler, consequently suppressing the precipitation of the filler and allowing the filler to fully adhere and spread in the composite. The modification of cellulose with CA improved the affinity of the filler, and the defibration enhanced the dispersibility of the filler. This has been reported previously by Habibi (2014) [42] that with modification on cellulose nanofibers, both the surface-area ratio and its chemical surface can improve the dispersibility as well as mechanical interlocking within the matrix.

3.3. Mechanical properties of CAC and F-CAC/Epoxy composites

The mechanical properties of the composites with cellulose, F-Cellulose, CAC, and F-CAC were evaluated using uniaxial tensile tests, as described previously (Table 2, Fig. 6). **Neat ER** exhibited Young's modulus of 1.07 GPa, maximum stress of 58.0 MPa, and elongation at break of 12.2 %.

Cellulose/ER showed an increase in Young's modulus and a decrease in maximum stress and elongation at break (51.3 MPa, 7.1 %) with the addition of rigid cellulose compared to **Neat ER**. The maximum stress was lower in **Cellulose/ER** because of the stress concentration caused by the nonuniform dispersion of cellulose in the composite.

With three different numbers of carboxyl groups in CAC, the composite with the lowest number of carboxyl groups, CAC-1.0 (**CAC-1.0/ER**), exhibited a higher Young's modulus than **Neat ER** and **Cellulose/ER**. Thus, it was confirmed that CAC had a better effect on improving mechanical properties than using cellulose. However, the nonuniform dispersion of CAC resulted in a lower maximum stress than **Neat ER**, and the elongation at break was similar to that of **Neat ER**. Composites with higher carboxyl group contents fillers (CAC-2.1 and CAC-2.7) showed a lower Young's modulus and similar maximum stress and elongation at break compared to **CAC-1.0/ER**, which can be attributed to the excess carboxyl groups in CAC impeding the formation of the epoxy network by epoxide and acid anhydride.

F-Cellulose/ER exhibited a higher Young's modulus, maximum stress, and lower elongation at break than that of **Cellulose/ER**. The maximum stress did not decrease and was 57.7 MPa, which was almost the same value as that of **Neat ER**. As the cellulose fibers decreased in diameter due to defibration, they were more dispersible in the matrix, as indicated in the SEM images. By defibrating CAC-1.0 to produce F-CAC-1.0 as the filler, the highest Young's modulus, maximum stress, and lowest elongation at break of **F-CAC-1.0/ER** were observed among other composites with a Young's modulus of 2.08 GPa, which was 1.9 times higher than that of **Neat ER**. The improved dispersibility of F-CAC caused by defibration resulted in an even greater improvement in mechanical properties than that of CAC. These results suggest that the modification with CA and defibration of cellulose improved the performances of cellulose as a filler for epoxy.

The effect of the amount of F-CAC-1.0 added (1, 3, 5, 10, or 15 wt %) on the overall mechanical properties of the composites were also evaluated (Table 3, Fig. 7a). From 1 to 5 wt %, there was a gradual increase in Young's modulus from 1.33 GPa, 2.00 GPa to 2.08 GPa and maximum stress with an increased filler amount. The elongation at break decreased at 3 and 5 wt % compared to 1 wt %. However, at 10 wt % and 15 wt % filler content, both Young's modulus and maximum stress dropped to 1.67 GPa, 59.4 MPa (10 wt %) and 1.07 GPa, 46.2 MPa (15 wt %), respectively. These results were less than that of the composite with 5 wt % F-CAC-1.0 filler. The elongation at break increased at 10 and 15 wt % compared to 5 wt %. In composites with filler contents of 10 wt % or more, the amount of filler powder is large relative to the reaction solution. Therefore, the solution mixed with filler before curing was less uniform, and the filler aggregated in the composites (Fig. 7b-d). Filler aggregation deteriorated the mechanical properties of composites with >10 wt % filler. Thus, the optimum amount of F-CAC-1.0 was 5 wt % because of its maximum mechanical properties, and this amount of filler was used in further experiments.

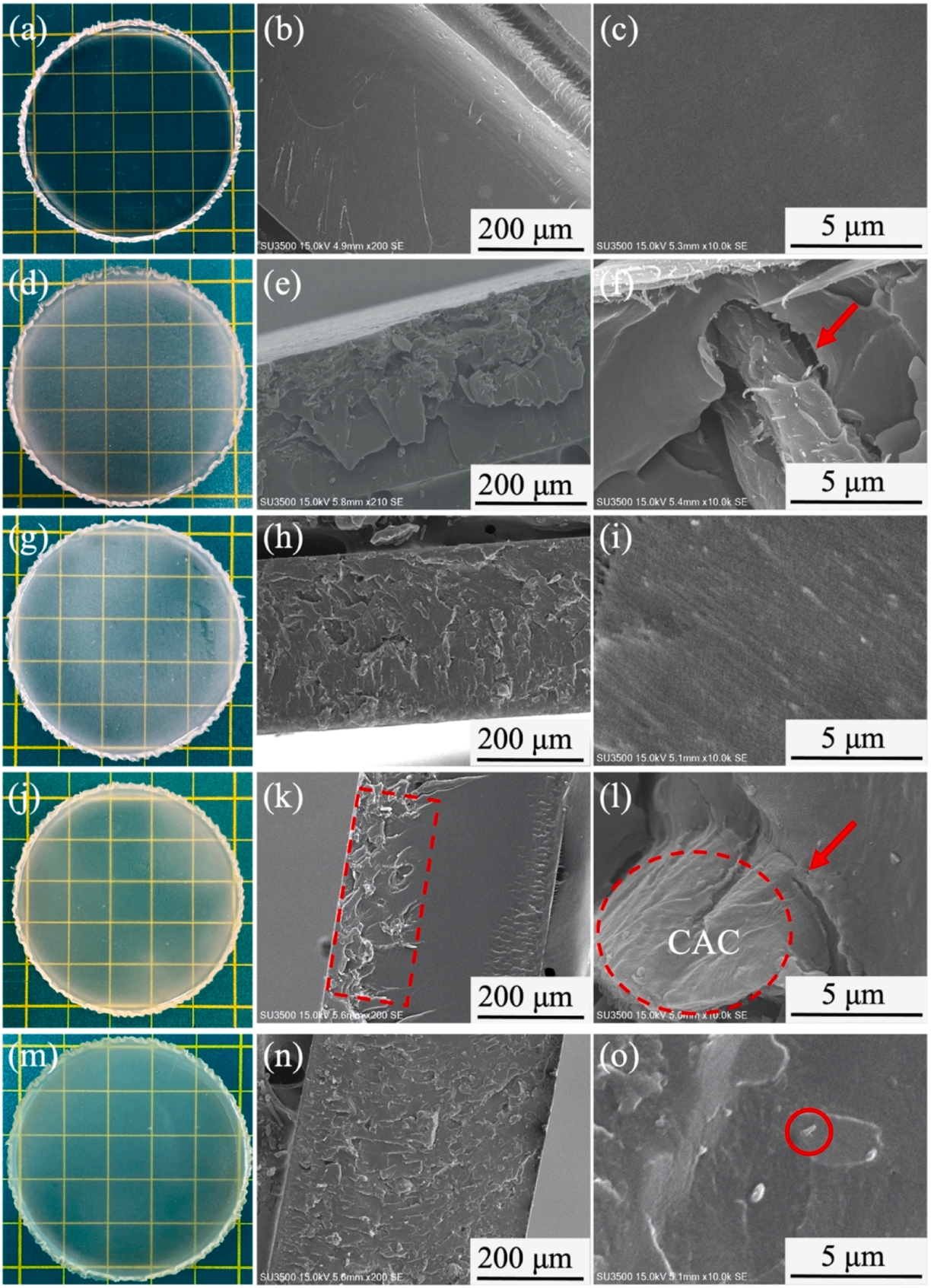

Fig. 5. Composites and SEM images of their cross sections (a–c) **Neat ER**, (d–f) **Cellulose/ER**, (g–i) **F-Cellulose/ER**, (j–l) **CAC/ER**, and (m–o) **F-CAC/ER**.

Table 2
Tensile test results of the composites.

	Young's modulus [GPa]	Maximum stress [MPa]	Elongation at break [%]
Neat ER	1.07 ± 0.11	58.0 ± 2.5	12.2 ± 1.4
Cellulose/ER	1.21 ± 0.05	51.3 ± 8.2	7.1 ± 1.3
F-Cellulose/ ER	1.43 ± 0.09	57.7 ± 3.4	5.9 ± 0.9
CAC-1.0/ER	1.56 ± 0.05	55.9 ± 5.0	11.9 ± 2.1
CAC-2.1/ER	1.08 ± 0.07	51.7 ± 7.8	7.6 ± 2.3
CAC-2.7/ER	1.17 ± 0.04	56.7 ± 4.8	10.8 ± 1.9
F-CAC-1.0/ ER	2.08 ± 0.10	69.8 ± 7.9	4.7 ± 0.3

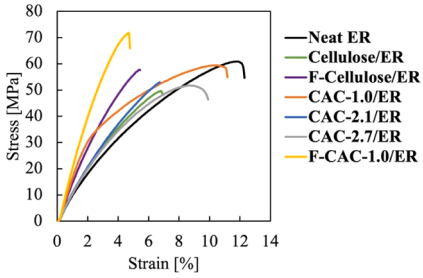

Fig. 6. Stress–strain curve of the tensile test.

Table 3
Tensile test results of **F-CAC-1.0/ER** with different additives.

F-CAC [wt %]	Young's modulus [GPa]	Maximum stress [MPa]	Elongation at break [%]
1	1.33 ± 0.07	60.6 ± 4.7	8.2 ± 0.4
3	2.00 ± 0.07	59.7 ± 2.7	4.1 ± 0.3
5	2.08 ± 0.10	69.8 ± 7.9	4.7 ± 0.3
10	1.67 ± 0.07	59.4 ± 3.7	7.4 ± 0.7
15	1.07 ± 0.01	46.2 ± 0.2	11.1 ± 0.6

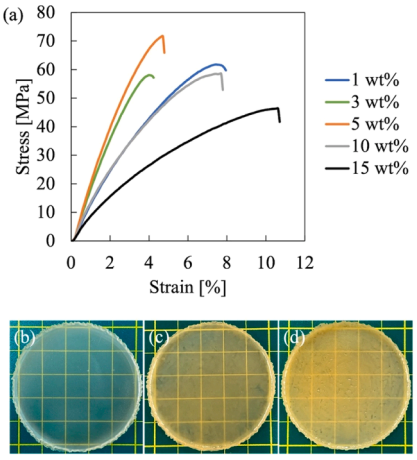

Fig. 7. (a)Stress–strain curves of **F-CAC-1.0/ER** with different additions. Pictures of **F-CAC-1.0/ER** (b) 5 wt %, (c) 10 wt %, (d) 15 wt %.

3.4. Thermal properties of composites

The viscoelasticity of **Neat ER, Cellulose/ER, F-Cellulose/ER, CAC-1.0/ER**, and **F-CAC-1.0/ER** at −30 °C to 130 °C was evaluated by DMA (Table 4, Fig. 8). The values of the storage modulus *E'* at 30 °C were higher for **CAC-1.0/ER** and **F-CAC-1.0/ER** than those for **Neat ER, Cellulose/ER**, and **F-Cellulose/ER**, which showed a correlation with

Table 4
Storage modulus (*E'*) at 30 °C, the maximum value of tanδ, glass transition temperature (T_g), and cross-linking density (*n*) at 90 °C of each composite.

(5 wt %)	*E'* (30 °C) [× 10^3 MPa]	tanδ	T_g [°C]	*n* (90 °C) [× 10^{-4} mol/cm^3]
Neat ER	2.45	1.89	56.0	5.7
Cellulose/ER	2.25	1.66	56.9	10.5
F-Cellulose/ER	2.44	1.17	54.9	8.7
CAC-1.0/ER	2.73	1.14	55.6	6.7
F-CAC-1.0/ER	2.60	1.35	57.8	13.5

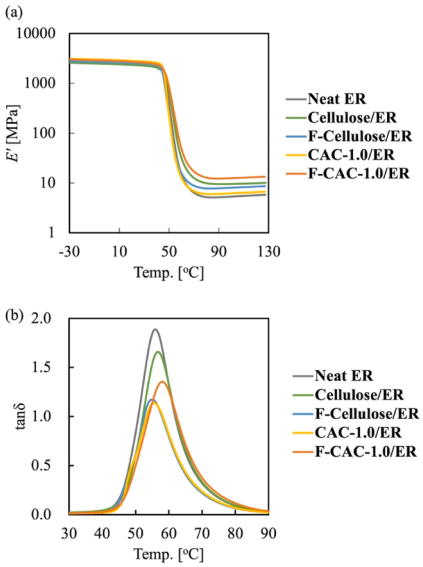

Fig. 8. Measurements of (a) storage modulus *E'* and (b) tanδ for each composite.

the mechanical properties (Fig. 8a). The cross-linking density *n* was calculated from the storage modulus *E'* in the rubber plateau range (Eq. (1)) [43,44]. *T* is the absolute temperature, and *R* is the gas constant. The *n* of **neat ER** represents the density of the network formed by epoxides and acid anhydrides. Due to the interaction between the filler and the matrix, the *n* of each composite was higher than that of **neat ER**. The *n* of **F-CAC-1.0/ER** exhibited the highest value, and it is hypothesized that this is attributable to the extensive interaction resulting from the superior dispersibility of the filler and the formation of bonds between the filler and epoxide. In **Cellulose/ER**, the interaction between cellulose fillers may be a contributing factor to the elevated *n*. The maximum value of tanδ was smaller for each composite than that for **Neat ER**, thereby confirming the increased elasticity of the composites (Fig. 8b). Furthermore, the peak top of tanδ yielded the glass transition temperature T_g (Table 4), which was close to that of **Cellulose/ER** and **CAC-1.0/ER.** A higher T_g was obtained for **F-CAC-1.0/ER** compared to that for **Neat ER**. It is suggested that when F-CAC with its excellent affinity and dispersibility was used as filler, numerous cross-linking reactions proceeded between the filler and the matrix. As a result, the formation of a strong network structure was inferred, and the T_g of the composite increased. Thus, the addition of F-CAC-1.0 improved the thermal properties of the composite.

$$n = \frac{E'}{3RT} \tag{1}$$

3.5. Schematic illustration

The possible mechanism behind the improvement in the filler performance is illustrated (Fig. 9), with a comparison between cellulose,

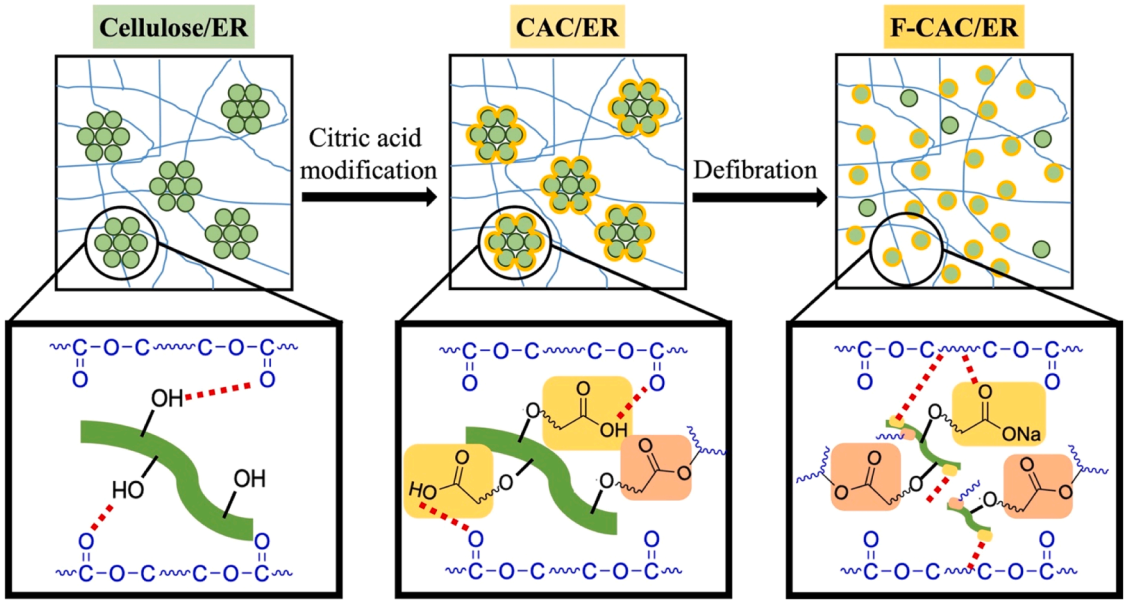

Fig. 9. Schematic of the filler action within composites.

CAC, and F-CAC in a network of epoxy. Although cellulose filler was aggregated within the composite, the strength of the composite improved because of the interactions between the hydroxyl groups of cellulose and the carboxyl oxygen in the epoxy network, which formed hydrogen bonds. While in CAC, the affinity between the matrix and the filler is improved compared to that of cellulose because the cellulose surface is modified with CA. The CA moiety interacts with the network via hydrogen bonding, and a new network can be formed between the carboxyl groups of CAC and the epoxides to further improve the strength of the composites. This reasoning also applies to F-CAC; however, with defibration, the filler can disperse better throughout the composite, promoting interaction and network formation in the composite and resulting in a significant improvement in its mechanical properties.

4. Conclusion

In this study, F-CAC was used as a filler to improve the mechanical and thermal properties of epoxy composites. CAC was easily prepared by mixing and heating cellulose and citric acid for esterification, and the number of introduced carboxyl groups could be controlled by heating conditions. Additionally, CAC was defibrated to prepare F-CAC, which has a smaller fiber diameter than CAC. Morphology observations of the composites confirmed that CAC has a higher affinity for matrix than cellulose and that F-CAC has improved dispersion in the composites. The Young's modulus in tensile tests of the composites with F-CAC increased approximately double that of epoxy without filler. The T_g of the composite with F-CAC, as measured by DMA, was higher than that of epoxy without filler. The postulated mechanism for improving the mechanical properties of CAC and F-CAC is hydrogen bonding between the carbonyl groups of CA and the epoxy network. Furthermore, the storage modulus by DMA indicates a high cross-linking density of the composites with CAC or F-CAC, suggesting that a cross-linking reaction between the carboxyl groups of CAC or F-CAC and epoxides may have progressed. This research contributes to sustainable development by providing a method to strengthen epoxy with a small environmental impact filler, citric acid modified and defibrated cellulose.

CRediT authorship contribution statement

Shotaro Yano: Writing – original draft, Methodology, Investigation, Conceptualization. **Yu-I Hsu:** Writing – review & editing, Supervision, Investigation, Funding acquisition, Conceptualization. **Hiroshi Uyama:** Writing – review & editing, Supervision, Funding acquisition, Conceptualization.

Declaration of competing interest

The authors declare that they have no known competing financial interests or personal relationships that could have appeared to influence the work reported in this paper.

Acknowledgments

This work was supported by Japan Science and Technology Agency (JST) PRESTO Grant Number JPMJPR23N4, the Core Research for Evolutional Science and Technology (CREST) program Grant Number JPMJCR24S5, the Environment Research and Technology Development Fund JPMEERF21S11900 of the Environmental Restoration and Conservation Agency of Japan, and Japan Society for the Promotion of Science (JSPS) KAKENHI Grants (22K21348 and 23K26717).

Data availability

No data was used for the research described in the article.

References

[1] H.Q. Pham and M.J. Marks, 2005. Epoxy resins. Ullmann's encyclopedia of industrial chemistry. https://doi.org/10.1002/14356007.a09_547.pub2.
[2] J.C. Capricho, B. Fox, N. Hameed, Multifunctionality in epoxy resins, Polymer Rev. 60 (2020) 1–41, https://doi.org/10.1080/15583724.2019.1650063.
[3] R. Dallaev, T. Pisarenko, N. Papež, P. Sadovský, V. Holcman, A brief overview on epoxies in electronics: properties, applications, and modifications, Polymers 15 (2023) 3964, https://doi.org/10.3390/polym15193964.
[4] I. Karlsson, D.J. Ponting, M.A. Ortega, I.B. Niklasson, L. Ndreu, E.J.L. Stéen, T. Seifert, K. Luthman, A.-T. Karlberg, Nature-derived epoxy resin monomers with reduced sensitizing capacity–Isosorbide-based bis-epoxides, Chem. Res. Toxicol. 36 (2023) 281–290, https://doi.org/10.1021/acs.chemrestox.2c00347.
[5] S. Caillol, From natural phenols to biobased epoxy resins, Rev. Fr. Allergol. 63 (2023) 103286, https://doi.org/10.1016/j.reval.2023.103286.
[6] H. Zhou, X. Fan, C. Liu, C. Qu, Z. Yuan, J. Jing, Y. Tang, D. Zhao, W. Xiao, K. Su, Properties of high-temperature epoxy/DDS resin systems for bonding application, High Perform. Polym. 32 (2020) 559–568, https://doi.org/10.1177/0954008319888002.
[7] E.O. Ozgul, M.H. Ozkul, Effects of epoxy, hardener, and diluent types on the workability of epoxy mixtures, Constr. Build. Mater. 158 (2018) 369–377, https://doi.org/10.1016/j.conbuildmat.2017.10.008.

[8] J.-M. Raquez, M. Deléglise, M.-F. Lacrampe, P. Krawczak, Thermosetting (bio) materials derived from renewable resources: a critical review, Prog. Polym. Sci. 35 (2010) 487–509, https://doi.org/10.1016/j.progpolymsci.2010.01.001.
[9] R. Auvergne, S. Caillol, G. David, B. Boutevin, J.-P. Pascault, Biobased thermosetting epoxy: present and future, Chem. Rev. 114 (2014) 1082–1115, https://doi.org/10.1021/cr3001274.
[10] C. Zhang, J. Xue, X. Yang, Y. Ke, R. Ou, Y. Wang, S.A. Madbouly, Q. Wang, From plant phenols to novel bio-based polymers, Prog. Polym. Sci. 125 (2022) 101473, https://doi.org/10.1016/j.progpolymsci.2021.101473.
[11] S. Bagheri, M. Nejad, Fully biobased composite made with epoxidized-lignin, reinforced with bamboo fibers, Polym. Compos. 44 (2023) 3926–3938, https://doi.org/10.1002/pc.27366.
[12] C. Noè, M. Hakkarainen, S. Malburet, A. Graillot, K. Adekunle, M. Skrifvars, M. Sangermano, Frontal-photopolymerization of fully biobased epoxy composites, Macromol. Mater. Eng. 307 (2022) 2100864, https://doi.org/10.1002/mame.202100864.
[13] J. Xu, X. Liu, S. Fu, Bio-based epoxy resin from gallic acid and its thermosets toughened with renewable tannic acid derivatives, J. Mater. Sci. 57 (2022) 9493–9507, https://doi.org/10.1007/s10853-022-07174-z.
[14] K. Sugane, T. Mishima, M. Shibata, Biobased epoxy nanocomposites composed of sorbitol polyglycidyl ether, biobased carboxylic acids and microfibrillated cellulose, J. Polymer Res. 28 (2021) 257, https://doi.org/10.1007/s10965-021-02595-x.
[15] B. Balanuca, R.S. Komartin, M.I. Necolau, C.M. Damian, R. Stan, Investigating the synthesis and characteristics of UV-cured bio-based epoxy vegetable oil-lignin composites mediated by structure-directing agents, Polymers 15 (2023) 439, https://doi.org/10.3390/polym15020439.
[16] R. Yang, W. Li, R. Mo, X. Zhang, Recyclable and degradable vinylogous urethane epoxy thermosets with tunable mechanical properties from isosorbide and vanillic acid, ACS Appl. Polym. Mater. 5 (2023) 2553–2561, https://doi.org/10.1021/acsapm.2c02186.
[17] W. Zhang, F. Gao, X. Chen, L. Shen, Y. Chen, Y. Lin, Recyclable, degradable, and fully bio-based covalent adaptable polymer networks enabled by a dynamic diacetal motif, ACS Sustain. Chem. Eng. 11 (2023) 3065–3073, https://doi.org/10.1021/acssuschemeng.2c06870.
[18] O.P. Korobeinichev, E.A. Sosnin, A.A. Shaklein, A.I. Karpov, A.R. Sagitov, S. A. Trubachev, A.G. Shmakov, A.A. Paletsky, I.V. Kulikov, The effect of flame-retardant additives DDM-DOPO and graphene on flame propagation over glass-Fiber-reinforced epoxy resin under the influence of external thermal radiation, Molecules 28 (2023) 5162, https://doi.org/10.3390/molecules28135162.
[19] V.E. Ogbonna, A.P.I. Popoola, O.M. Popoola, A review on recent advances on the mechanical and conductivity properties of epoxy nanocomposites for industrial applications, Polymer Bull. 80 (2023) 3449–3487, https://doi.org/10.1007/s00289-022-04249-4.
[20] X. Zhang, X. Fan, C. Yan, H. Li, Y. Zhu, X. Li, L. Yu, Interfacial microstructure and properties of carbon fiber composites modified with graphene oxide, ACS Appl. Mater. Interfaces 4 (2012) 1543–1552, https://doi.org/10.1021/am201757v.
[21] R.M. Neves, H.L. Ornaghi, A.J. Zattera, S.C. Amico, Recent studies on modified cellulose/nanocellulose epoxy composites: a systematic review, Carbohydr. Polym. 255 (2021) 117366, https://doi.org/10.1016/j.carbpol.2020.117366.
[22] K. Gardner, J. Blackwell, The hydrogen bonding in native cellulose, Biochim. et Biophys. Acta (BBA) - General Sub. 343 (1974) 232–237, https://doi.org/10.1016/0304-4165(74)90256-6.
[23] M. Jakob, A.R. Mahendran, W. Gindl-Altmutter, P. Bliem, J. Konnerth, U. Müller, S. Veigel, The strength and stiffness of oriented wood and cellulose-fibre materials: a review, Prog. Mater. Sci. 125 (2022) 100916, https://doi.org/10.1016/j.pmatsci.2021.100916.
[24] T. Heinze, Cellulose: structure and properties. Cellulose chemistry and properties: fibers, Nanocellul. Adv. Mater. 271 (2015) 1–52, https://doi.org/10.1007/12_2015_319.
[25] S. Alexander, M. Alidu, Recovery of cellulose from food and agricultural waste, Cellulose - Biobased Solut. Soc. (2025), https://doi.org/10.5772/intechopen.1009308.
[26] A. Masek, A. Kosmalska, Technological limitations in obtaining and using cellulose biocomposites, Front Bioeng. Biotechnol. 10 (2022) 912052, https://doi.org/10.3389/fbioe.2022.912052.
[27] J. Lu, P. Askeland, L.T. Drzal, Surface modification of microfibrillated cellulose for epoxy composite applications, Polymer 49 (2008) 1285–1296, https://doi.org/10.1016/j.polymer.2008.01.028.
[28] T. Saito, S. Kimura, Y. Nishiyama, A. Isogai, Cellulose nanofibers prepared by TEMPO-mediated oxidation of native Cellulose, Biomacromolecules 8 (2007) 2485–2491, https://doi.org/10.1021/bm0703970.
[29] E. Abraham, D. Kam, Y. Nevo, R. Slattegard, A. Rivkin, S. Lapidot, O. Shoseyov, Highly modified cellulose nanocrystals and formation of epoxy-nanocrystalline cellulose (CNC) nanocomposites, ACS Appl. Mater. Interfaces 8 (2016) 28086–28095, https://doi.org/10.1021/acsami.6b09852.
[30] A. Isogai, T. Saito, H. Fukuzumi, TEMPO-oxidized cellulose nanofibers, Nanoscale 3 (2011) 71–85, https://doi.org/10.1039/C0NR00583E.
[31] J.L. Sanchez-Salvador, H. Xu, A. Balea, A. Blanco, C. Negro, Enhancement of the production of TEMPO-mediated oxidation cellulose nanofibrils by kneading, Int. J. Biol. Macromol. 261 (2024) 129612, https://doi.org/10.1016/j.ijbiomac.2024.129612.
[32] D. Bondeson, A. Mathew, K. Oksman, Optimization of the isolation of nanocrystals from microcrystalline cellulose by acid hydrolysis, Cellulose 13 (2006) 171–180, https://doi.org/10.1007/s10570-006-9061-4.
[33] M. Mariano, N. El Kissi, A. Dufresne, Cellulose nanocrystals and related nanocomposites: review of some properties and challenges, J. Polym. Sci. B: Polym. Phys. 52 (2014) 791–806, https://doi.org/10.1002/polb.23490.
[34] S. Ma, D.C. Webster, Naturally occurring acids as cross-linkers to yield VOC-free, high-performance, fully bio-based, degradable thermosets, Macromolecules 48 (2015) 7127–7137, https://doi.org/10.1021/acs.macromol.5b01923.
[35] S. Kocaman, G. Ahmetli, M. Temiz, Newly epoxy resin synthesis from citric acid and the effects of modified almond shell waste with different natural acids on the creation of bio-based composites, Ind. Crops. Prod. 220 (2024) 119106, https://doi.org/10.1016/j.indcrop.2024.119106.
[36] I. Romeo, F. Olivito, A. Tursi, V. Algieri, A. Beneduci, G. Chidichimo, L. Maiuolo, E. Sicilia, A. De Nino, Totally green cellulose conversion into bio-oil and cellulose citrate using molten citric acid in an open system: synthesis, characterization and computational investigation of reaction mechanisms, RSC Adv. 10 (2020) 34738–34751, https://doi.org/10.1039/d0ra06542k.
[37] J.A. Ávila Ramírez, E. Fortunati, J.M. Kenny, L. Torre, M.L. Foresti, Simple citric acid-catalyzed surface esterification of cellulose nanocrystals, Carbohydr. Polym. 157 (2017) 1358–1364, https://doi.org/10.1016/j.carbpol.2016.11.008.
[38] X. Cui, A. Ozaki, T.-A. Asoh, H. Uyama, Cellulose modified by citric acid reinforced poly(lactic acid) resin as fillers, Polym. Degrad. Stab. 175 (2020) 109118, https://doi.org/10.1016/j.polymdegradstab.2020.109118.
[39] X. Cui, T. Honda, T.-A. Asoh, H. Uyama, Cellulose modified by citric acid reinforced polypropylene resin as fillers, Carbohydr. Polym. 230 (2020) 115662, https://doi.org/10.1016/j.carbpol.2019.115662.
[40] K.K. Mali, S.C. Dhawale, R.J. Dias, N.S. Dhane, V.S. Ghorpade, Citric acid crosslinked carboxymethyl cellulose-based composite hydrogel films for drug delivery, Indian J. Pharm. Sci. 80 (2018) 657–667, https://doi.org/10.4172/pharmaceutical-sciences.1000405.
[41] N. Masruchin, B.-D. Park, Manipulation of surface carboxyl content on TEMPO-oxidized cellulose fibrils, J. Korean Wood Sci. Technol. 43 (2015) 613–627, https://doi.org/10.5658/WOOD.2015.43.5.613.
[42] Y. Habibi, Key advances in the chemical modification of nanocelluloses, Chem. Soc. Rev. 43 (2014) 1519–1542, https://doi.org/10.1039/C3CS60204D.
[43] M. Zajac, H. Kahl, B. Schade, T. Rödel, M. Dionisio, M. Beiner, Relaxation behavior of polyurethane networks with different composition and crosslinking density, Polymer 111 (2017) 83–90, https://doi.org/10.1016/j.polymer.2017.01.032.
[44] J.-H. Cai, M.-L. Huang, X.-D. Chen, M. Wang, Controllable construction of cross-linking network for regulating on the mechanical properties of polydimethylsiloxane and polydimethylsiloxane/carbon nanotubes composites, J. Appl. Polym. Sci. 139 (2022) 52113, https://doi.org/10.1002/app.52113.